SCIENCE CHINA
Physics, Mechanics & Astronomy

• Research Paper •

December 2011 Vol.54 No.12: 2196–2201
doi: 10.1007/s11433-011-4500-0

Elastic and thermodynamic properties of TiC from first-principles calculations

LI YanHong[1], WANG WanFeng[1], ZHU Bo[1], XU Ming[1], ZHU Jun[1,2*], HAO YanJun[1*], LI WeiHu[1] & LONG XiaoJiang[1]

[1] *College of Physical Science and Technology, Sichuan University, Chengdu 610064, China;*
[2] *Institute of Atomic and Molecular Physics, Sichuan University, Chengdu 610065, China*

Received April 20, 2011; accepted May 13, 2011; published online October 26, 2011

Using the pseudopotential plane-wave method, we investigate the elastic constants and thermodynamic properties of the rock-salt structure Titanium Carbide (TiC). The obtained lattice parameters, bulk modulus and elastic constants are in very good agreement with the available experimental data and other theoretical results. The thermodynamic properties of the cubic TiC are predicted by using the quasi-harmonic Debye model. The normalized volume V/V_0, bulk modulus B, thermal expansion α, heat capacity C_V, Grüneisen parameter γ and Debye temperature Θ dependence on the pressure and temperature are obtained successfully. At low temperature and low pressure, thermal expansion coefficient increases rapidly with temperature. At high temperature and high pressure, the increasing trend becomes tender. At low temperatures, C_V is proportional to T^3, and C_V tends to the Dulong-Petit limit at higher temperatures.

thermodynamic properties, elastic constants, TiC

PACS: 65.40.-b, 62.20.Dc, 72.80.Ga

1 Introduction

As one of the transition-metal carbides, Titanium Carbide (TiC) is widely used as the main constituent in metal cutting tools and coating materials for surface protection due to its extreme hardness, high melting temperature and excellent corrosion resistance [1,2]. In addition, TiC is an important constituent and strengthening phase for nickel-base super alloys, metal matrix composites (MMCs) and intermetallic matrix composites (IMCs), and can dramatically improve the mechanical performance of these materials [3]. Therefore, it is of great interests to physicists in experimental [4−7] and theoretical [2,8−12] investigations of TiC.

X-ray diffraction experiment by Houska [4] showed that the vibration amplitude of nearly stoichiometric TiC generally increased with thermal expansion at T>2000°C. Dodd et al. [5] measured the dependences of the elastic stiffness moduli and related elastic properties for TiC on temperature in the range of 135–295 K and hydrostatic pressure up to 0.2 GPa using the pulse-echo overlap measurements of ultrasonic wave velocity technology. Dubrovinskaia et al. [6] observed a phase transformation from the NaCl-type cubic structure (B1) to a rhombohedral structure at a pressure above 18 GPa at 300 K under a quasi-hydrostatic environment using *in situ* powder X-ray diffraction. However, Winkler et al. [7] found that TiC did not undergo a structural phase transition up to 25 GPa from a laser-heated diamond anvil cell experiment.

Theoretically, the vibrational spectrum for TiC was studied by using molecular dynamics simulation method [8]. Mécabih et al. [9] calculated the structural and optical properties of TiC by using the full potential-linear augmented plane wave (FP-LAPW) method. Dridi et al. [10] studied

*Corresponding author (email: zhujun@scu.edu.cn; haoyanjun@scu.edu.cn)

the effect of vacancies on the structural and electronic properties in substoichiometric TiC_x using a full-potential linear augmented plane-wave (FP-LAPW) method. Kim et al. [2] employed modified embedded-atom method (MEAM) to investigate the fundamental physical properties–structural properties (enthalpy of formation, lattice parameter and dilute heat of solution), elastic properties (bulk modulus, elastic constants), thermal properties (thermal linear expansion, melting points) of TiC. Yang et al. [11] and Jochym et al. [12] investigated the elastic properties and phonon dispersion curves of TiC by using pseudopotential plane wave method, respectively.

On the other hand, elastic properties relate to various fundamental solid-state phenomena, such as interatomic potentials, equations of state, phonon spectra, and so on. Moreover, they are also associated with specific heat, thermal expansion, Debye temperature and Grüneisen parameter. The knowledge of elastic constants is essential for many practical applications related to the mechanical properties of a solid: load deflection, thermoelastic stress, internal strain, sound velocities, and fracture toughness [13].

Up to now, a few theoretical methods have been applied to the calculation of the elastic constants of TiC, such as the modified embedded-atom method (MEAM) [2], the first-principles plane wave in the scheme of generalized gradient approximation (GGA) [11] and local density approximation (LDA) [12], and the hybrid full-potential augmented plane-wave plus local orbitals method [14]. In this work, we focus on investigating the elastic constants and the thermodynamic properties of TiC by the plane-wave pseudo potential density function theory (DFT) method [15,16]. The results obtained are in good agreement with the available experimental results and other theoretical data.

This paper is organized as follows: in sect. 2, we have a brief review of the theoretical methods, and in sect. 3 the calculated results are discussed carefully compared with the previous theoretical and experimental results. Finally, we get some conclusions in sect. 4.

2 Theoretical methods

2.1 Total energy electronic structure calculations

The electronic structure total energy calculations are implemented based on the DFT, the exchange and correlation potentials are treated within the GGA in the scheme of Perdew-Burke-Ernzerhof (PBE) [17]. The electronic wave functions are expanded in a plane wave basis set with energy cut-off 1230 eV. The pseudo-atomic calculations are performed for Ti ($3s^2 3p^6 3d^2 4s^2$) and C ($2s^2 2p^2$). For the Brillouin-zone k-point sampling, we use the 19×19×19 Monkhorst-Pack mesh, where the self-consistent convergence of the total energy is 1×10^{-6} eV/atom. All the total energy electronic structure calculations are implemented through the Cambridge Serial Total Energy Package (CASTEP) program [18].

2.2 Thermodynamic properties

To study the thermodynamic properties of the rock-salt (RS) TiC, we apply the quasi-harmonic Debye model [19], in which the non-equilibrium Gibbs function $G^*(V;P,T)$ takes the form of

$$G^*(V;P,T) = E(V) + PV + A_{\rm vib}(\Theta(V);T), \tag{1}$$

where $E(V)$ is the total energy, PV corresponds to the constant hydrostatic pressure condition, $\Theta(V)$ is the Debye temperature, and the vibrational Helmholtz free energy $A_{\rm vib}$ can be written as [20,21]

$$A_{\rm vib}(\Theta(V);T) = nKT\left[\frac{9}{8}\frac{\Theta}{T} + 3\ln(1-{\rm e}^{\Theta/T}) - D\left(\frac{\Theta}{T}\right)\right], \tag{2}$$

where $D(\Theta/T)$ represents the Debye integral, n is the number of atoms per formula unit. For an isotropic solid, Θ is expressed by [21]

$$\Theta = \frac{\hbar}{\kappa}(6\pi^2 V^{1/2} n)^{1/3} f(\sigma)\sqrt{\frac{B_{\rm s}}{M}}, \tag{3}$$

where M is the molecular mass per formula unit, $B_{\rm S}$ is the adiabatic bulk modulus approximated by the static compressibility [19]

$$B_{\rm S} \approx B(V) = V\left[\frac{{\rm d}^2 E(V)}{{\rm d}V^2}\right]. \tag{4}$$

$f(\sigma)$ is given by ref. [22]:

$$f(\sigma) = \left\{3\left[2\left(\frac{2}{3}\frac{1+\sigma}{1-\sigma}\right)^{3/2} + \left(\frac{1}{3}\frac{1+\sigma}{1-\sigma}\right)^{3/2}\right]^{-1}\right\}^{1/3}. \tag{5}$$

The Poisson ratio σ is taken as 0.199 [23]. Therefore, the non-equilibrium Gibbs function $G^*(V; P, T)$ as a function of $(V; P, T)$ can be minimized with respect to volume V

$$\left(\frac{\partial G^*(V;P,T)}{\partial V}\right)_{P,T} = 0. \tag{6}$$

By solving eq. (6), the thermal equation of state (EOS) $V(P,T)$ may be obtained. The isothermal bulk modulus B_T and the heat capacity C_V are given by [23]

$$B_T(P,T) = V\left(\frac{\partial^2 G^*(V;P,T)}{\partial^2 V}\right)_{P,T}, \tag{7}$$

$$C_V = 3n\kappa\left[4D(\Theta/T) - \frac{3\Theta/T}{{\rm e}^{\Theta/T}-1}\right], \tag{8}$$

$$\alpha = \frac{\gamma C_V}{B_T V}, \tag{9}$$

where γ is the Grüneisen parameter, which is defined as

$$\gamma = -\frac{\mathrm{d}(\ln \Theta(V))}{\mathrm{d}(\ln(V))}. \quad (10)$$

We have successfully studied the thermodynamic properties of some materials [24–26] using these methods described above.

3 Results and discussion

To obtain the equilibrium structure parameters of RS-TiC, a series of different primitive cell volume V are set to calculate the total energies E and then the calculated energy-volume (E-V) points are fitted to the Brich-Murnaghan EOS [27]. The obtained lattice constant a, the bulk modulus B_0 and the first order pressure derivatives of bulk modulus B'_0 are listed in Table 1. Obviously, the obtained results are in good agreement with the available experimental data [5,23,28–30] and other theoretical results [2,9–11,14]. Moreover, we also calculate the adiabatic bulk B_S and the shear modulus G, which are given by

$$B_S = \left(C_{11} + 2C_{12}\right)/3, \quad (11)$$

$$G = \frac{1}{2}\left(G_R + G_V\right), \quad (12)$$

where $G_V=(C_{11}-C_{12}+3C_{44})/5$, $G_R=5(C_{11}-C_{12})C_{44}/[4C_{44}+3(C_{11}-C_{12})]$, G_V is the Voigt shear modulus and G_R is the Reuss shear modulus. The adiabatic bulk B_S and the shear modulus G are also listed in Table 1, and these results are consistent with the experimental values [5,23].

Now, we turn to investigating the thermodynamic properties for RS-TiC by using the quasi-harmonic Debye model [19]. Figure 1 presents the pressure and temperature dependences of the normalized volume V/V_0, where V_0 is the equilibrium cell volume at zero pressure and zero temperature. It is seen that as the pressure increases, the relative volume V/V_0 decreases at a given temperature, and the relative volume V/V_0 of higher temperature is less than that of lower temperature at the same pressure. We also found that the volume V decreases with the increase of the pressure P, and decreases with the increase of the temperature T.

Figure 2 illustrates the relationships between the bulk

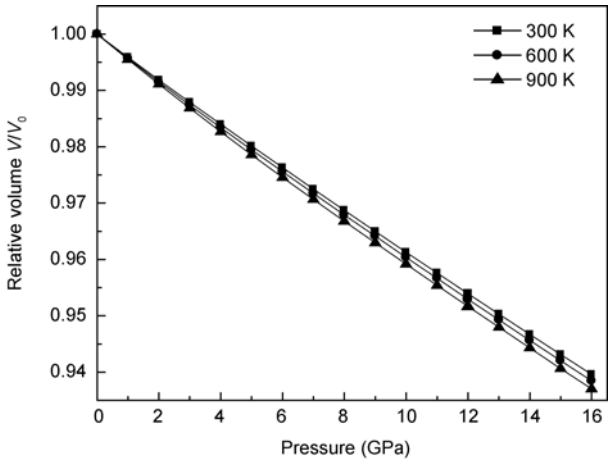

Figure 1 Calculated relative volume V/V_0 as a function of pressure for TiC at 300, 600 and 900 K, respectively.

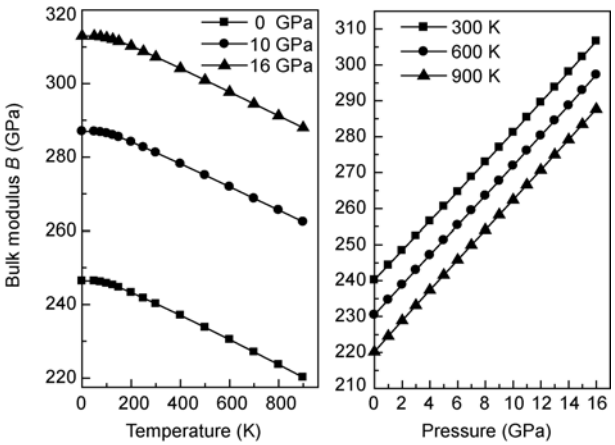

Figure 2 Pressure and temperature dependence on the bulk modulus of TiC.

Table 1 Lattice constant (Å), bulk modulus (GPa), and its pressure derivation of bulk modulus, elastic constant (GPa), the adiabatic bulk B_S (GPa) and the shear modulus G (GPa) of RS-TiC at zero pressure, compared with experimental and other theoretical data

	Present work	Other calc.	Exp.
a	4.33	4.33 [a], 4.42 [b], 4.35 [c], 4.28 [d], 4.27 [j]	4.33 [g], 4.328 [h]
B	244	249 [a], 242 [b], 273 [c], 277 [d], 281 [j]	242 [e], 240 [g]
B'_0	4.03	4.30 [c], 4.11 [d]	–
C_{11}	510	519 [a], 522 [b], 603 [j]	500 [e], 513 [i]
C_{12}	119	115 [a], 102[b], 103 [j]	113 [e], 106 [i]
C_{44}	168	183 [a], 129 [b], 191 [j]	175 [e], 178 [i]
B_S	250	–	233 [f]
G	179	190 [a]	182 [e], 184 [f]

a) ref. [11], b) ref. [2], c) ref. [9], d) ref. [10], e) ref. [23], f) ref. [5], g) ref. [28], h) ref. [29], i) ref. [30], j) ref. [14]

modulus with pressure P and temperature T. It is found that the bulk modulus B almost increases linearly with the applied P at different temperatures. At low temperature, the bulk modulus is close to a constant, but it drops remarkably at higher temperature, the reason of which is that the volume V increases with the increase of temperature T. It is also noted that the influences of the pressure on the bulk modulus are much more important than that of the temperature on it.

The variations of the thermal expansion α with temperature and pressure are depicted in Figure 3. It is observed that the thermal expansion increases rapidly with T^3 at low temperature and gradually approaches to almost a linear increase at high temperature, and then the increasing trend becomes gentler. As the pressure increases, the increase of α with temperature becomes smaller, especially at higher temperatures. At a given temperature, α decreases monotonically with increasing pressure. It is shown from Figure 3 that the temperature dependence of α is a little greater at higher temperatures and higher pressures. At the same time we also calculate the linear thermal expansion parameters α_l in the intralayer and interlayer directions at zero pressure. Through the following equation:

$$\alpha_l = \frac{(\Delta l/\Delta T)}{l_0} = \frac{1}{l_0}\frac{\partial l}{\partial T}\bigg|_P, \tag{13}$$

where l represents the lattice constants a, by fitting the l-T data to second-order polynomials as follows:

$$\alpha_l(T) = 4.33975 + 1.89424\times10^{-5}T + 2.21471\times10^{-8}T^2, \quad (P = 0\ \text{GPa}), \tag{14}$$

$$\alpha_l(T) = 4.31148 + 1.71563\times10^{-5}T + 2.01983\times10^{-8}T^2, \quad (P = 5\ \text{GPa}), \tag{15}$$

$$\alpha_l(T) = 4.28398 + 1.62945\times10^{-5}T + 1.94289\times10^{-8}T^2, \quad (P = 10\ \text{GPa}), \tag{16}$$

$$\alpha_l(T) = 4.25719 + 1.51243\times10^{-5}T + 1.92739\times10^{-8}T^2, \quad (P = 15\ \text{GPa}). \tag{17}$$

The obtained linear thermal expansion coefficient α_l is 7.43×10^{-6} K^{-1} at 300 K, which is well consistent with X-ray diffraction measurement, which yields thermal expansion coefficient 7.23×10^{-6} K^{-1} [31].

In Table 2, we list the calculated heat capacity at constant volume C_V, heat capacity at constant pressure C_P, Debye

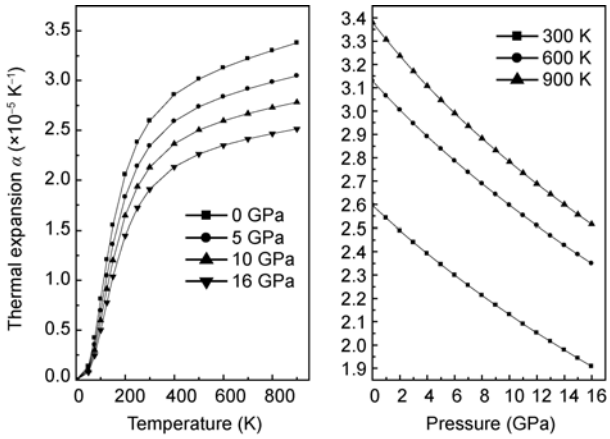

Figure 3 The thermal expansion versus pressure and temperature, respectively.

Table 2 The calculated heat capacity C_V and C_P (J·mol^{-1}·K^{-1}), Debye temperature Θ (K) and Grüneisen parameter γ for the cubic TiC at different pressures and temperatures

T (K)	P (GPa)	0	4	8	12	16
0	C_V	0.000	0.000	0.000	0.000	0.000
	C_P	0.000	0.000	0.000	0.000	0.000
	Θ	599.97	617.68	635.13	652.45	669.66
	γ	1.860	1.821	1.785	1.752	1.722
300	C_V	41.295	40.837	40.384	39.929	39.473
	C_P	41.896	41.373	40.865	40.362	39.864
	Θ	595.35	613.37	631.00	648.50	665.87
	γ	1.870	1.830	1.794	1.760	1.728
600	C_V	47.589	47.446	47.305	47.163	47.018
	C_P	49.281	48.968	48.688	48.424	48.173
	Θ	585.65	604.30	622.11	639.74	657.25
	γ	1.893	1.850	1.812	1.776	1.744
900	C_V	48.884	48.816	48.751	48.685	48.618
	C_P	51.739	51.373	51.068	50.800	50.557
	Θ	574.90	594.28	612.49	630.24	647.85
	γ	1.920	1.873	1.832	1.795	1.761

temperature Θ, and Grüneisen parameter γ for the RS-TiC at different pressures P (0, 4, 8, 12 and 16 GPa) and temperatures T (0, 300, 600 and 900 K). The calculated Debye temperature at T=300 K is 595.35 K, which is in reasonable agreement with the experimental value of 604.00 K [29]. It is found that from Table 2, when the applied pressure increases from 0 to 16 Gpa, the heat capacity C_V decreases by 4.41%, 1.20%, 0.54%, respectively, while the Debye temperature increases by 11.85%, 12.23%, 12.69% at temperatures of 300, 600 and 900 K. It is clear that, as the pressure increases, the heat capacity decreases more quickly at low temperature than at high temperature, but the Debye temperature is on the contrary trend. As an important physical quantity, The Grüneisen parameter characterizes the anharmonic properties of solids. From Table 2, we can also see that the Grüneisen parameter γ decreases with increasing pressure at a given temperature, and increases with increasing temperature at a given pressure.

Finally, the calculated heat capacity C_V at different pressures P and temperatures T are plotted in Figure 4. It is found that when T<600 K, the heat capacity C_V is dependent on both temperature T and pressure P. This is due to the anharmonic approximations. However, at higher temperatures and higher pressures, the anharmonic effect on heat capacity C_V is suppressed, and C_V is close to the Dulong-Petit limit $3k_B$ ($\approx$49.90 J·mol^{-1}·K^{-1}), which is common for all solids at high temperatures.

4 Conclusion

In summary, we have employed the first-principles plane wave method to investigate the elastic constants and thermodynamic properties of the RS-TiC. The calculated lattice parameters and elastic constants are well consistent with the available experimental data and other calculations. Through the quasi-harmonic Debye model, the thermodynamic properties including the normalized volume V/V_0, bulk modulus B, thermal expansion α, heat capacity C_V, Grüneisen constant γ and Debye temperature Θ dependence on the pressure and temperature are predicted systematically. The linear thermal expansion coefficient α_l in the intralayer and interlayer directions is also calculated. At zero pressure, the linear thermal expansion coefficient is 7.43×10^{-6} K^{-1} at 300 K and is in good agreement with the experimental data.

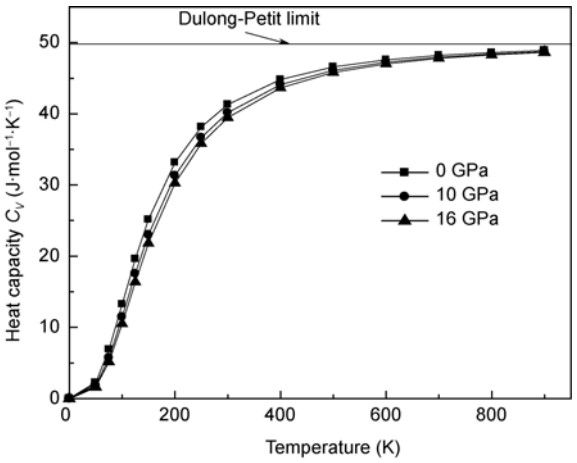

Figure 4 The dependence of heat capacity C_V on temperature for RS-TiC at 0, 10 and 16 GPa, respectively.

The authors gratefully acknowledge the support from the Fundamental Research Funds for the Central Universities (Grant No. 2009SCU11124).

1 Price D L, Cooper B R, Wills J M. Full-potential linear-muffin-tin-orbital study of brittle fracture in titanium carbide. Phys Rev B, 1992, 46: 11368–11375
2 Kim Y M, Lee B J. Modified embedded-atom method interatomic potentials for the Ti-C and Ti-N binary systems. Acta Mater, 2008, 56: 3481–3489
3 Chen Y, Wang H M. Growth morphologies and mechanism of TiC in the laser surface alloyed coating on the substrate of TiAl intermetallics. J Alloys Compd, 2003, 351: 304–308
4 Houska C R. Thermal expansion and atomic vibration amplitudes for TiC, TiN, ZrC, ZrN, and pure tungsten. J Phys Chem Solids, 1964, 25: 359–366
5 Dodd S P, Cankurtaran M, James B. Ultrasonic determination of the elastic and nonlinear acoustic properties fo transition-metal carbide ceramics: TiC and TaC. J Mater Sci, 2003, 38: 1107–1115
6 Dubrovinskaia N A, Dubrovinsky L S, Saxena S K, et al. High-pressure study of titanium carbide. J Alloys Compd, 1999, 289: 24–27
7 Winkler B, Juarez-Arellano E A, Friedrich A, et al. Reaction of titanium with carbon in a laser heated diamond anvil cell and reevaluation of a proposed pressure-induced structural phase transition of TiC. J Alloys Compd, 2009, 478: 392–397
8 Postnikov A V, Entel P. *Ab initio* simulations of Fe and TiC clusters. Phase Transitions, 2004, 77: 149–159
9 Mécabih S, Amrane N, Nabi Z, et al. Description of structure and electronic properties of TiC and ZrC by generalized gradient approximation. Phys A, 2000, 285: 392–396
10 Dridi Z, Bouhafs B, Ruterana P, et al. First-principles calculations of vacancy effects on structural and electronic properties of TiC_x and TiN_x. J Phys-Condes Matter, 2002, 14: 10237–10248
11 Yang Y, Lu H, Yu C, et al. First-principles calculations of mechanical properties of TiC and TiN. J Alloys Compd, 2009, 485: 542–547
12 Jochym P T, Parlinski K, Sternik M. TiC lattice dynamics from *ab initio* calculations. Eur Phys J B, 1999, 10: 9–13
13 Louail L, Maouche D, Roumili A, et al. Calculation of elastic constants of 4d transition metals. Mater Lett, 2004, 58: 2975–2978
14 Zaoui A, Bouhafs B, Ruterana P. First-principles calculations on the electronic structure of TiC_xN_{1-x}, $Zr_xNb_{1-x}C$ and HfC_xN_{1-x} alloys. Mater Chem Phys, 2005, 91: 108–115
15 Hohenberg P, Kohn W. Inhomogeneous electron gas. Phy Rev B, 1964, 136: 64–871
16 Kohn W, Sham L J. Self-consistent equations including exchange and correlation effects. Phys Rev A, 1965, 140: 1133–1138
17 Perdew J P, Chevary J A, Vosko S H, et al. Atoms, molecules, solids, and surfaces: Applications of the generalized gradient approximation for exchange and correlation. Phys Rev B, 1992, 46: 6671–6687
18 Payne M C, Teter M P, Allen D C, et al. Iterative minimization techniques for *ab initio* total-energy calculations: Molecular dynamics and conjugate gradients. Rev Mod Phys, 1992, 64: 1045–1097; Milan V, Winker B, White J A, et al. Electronic structure, properties, and phase stability of inorganic crystals: A pseudopotential plan-wave study. Int J Quantum Chem, 2000, 77: 895–910
19 Blanco M A, Francisco E, Luana V. GIBBS: Isobaric thermodynam-

ics of solids from energy curves using a quasi-harmonic Dybey model. Comput Phys Commun, 2004, 158: 57–72
20 Flòrez M, Recio J M, Francisco E, et al. First-principles study of the rocksalt-cesium chloride relative phase stability in alkali halides. Phys Rev B, 2002, 66: 144112–144120
21 Blanco M A, Pendás A M, Francisco E. Thermodynamical properties of solids from microscopic theory: Applications to MgF_2 and Al_2O_3. J Mol Struct (Theochem), 1996, 368: 245–255
22 Gilman J J, Roberts B W. Elastic constants of TiC and TiB_2. J Appl Phys, 1961, 32: 1405–1407
23 Francisco E, Blanco M A, Sanjurjo G. Atomistic simulation of SrF_2 polymorphs. Phys Rev B, 2001**,** 63: 094107–094115
24 Lu L Y, Cheng Y, Chen X R, et al. Thermodynamic properties of MgO under high pressure from first-principles calculations. Physica B, 2005, 370: 236–242
25 Chang J, Chen X R, Zhang W, et al. First-principles investigations on elastic and thermodynamic properties of zinc-blende structure BeS. Chin Phys B, 2008, 17: 1377–1381
26 Zhu J, Zhu B, Qu J Y, et al. Thermodynamic properties of cubic ZrC under high pressure from first-principles calculations. Sci China Ser G-Phys Mech Astron, 2009, 52: 1039–1042
27 Murnaghan F D. The compressibility of media under extreme pressures. Proc Natl Acad Sci USA, 1944, 30: 244–247
28 Holliday J E. Advance in X-ray Analysis. New York: Plenum Press, 1970. 13: 136
29 Christensen A N. The temperature factor parameters of some transition metal carbides and nitrides by single crystal X-Ray and neutron diffraction. Acta Chen Scand A, 1978, 32: 89–90
30 Choy M M, Cook W R, Hearmon R E S, et al. Numerical Data and Functional Relationships in Science and Technology, Elastic, Piezoelectric, Pyroelectric, Piezooptic, Electrooptic Constants, and Nonlinear Dielectric Susceptibilities of Crystals. Berlin: Springer Press, 1979
31 Elliott R O, Kempter C P. Thearmal expansion of some transition metal carbides. J Phys Chem, 1958, 62: 630–631